Microphysics of electrons at plasma boundaries

F. X. Bronold, H. Fehske, and H. Deutsch

Institut für Physik, Ernst-Moritz-Arndt-Universität Greifswald, D-17489 Greifswald, Germany

Abstract: We present a physisorption-inspired quantum-kinetic description of the microphysics of electrons at plasma boundaries which is responsible for the build-up of surface charges. Specifically, we calculate the electron sticking coefficient s_e and the electron desorption time τ_e for metallic boundaries assuming external image states and electron-hole pairs in the metal to control energy relaxation, and thus physisorption, of electrons at metallic boundaries. The sticking coefficient turns out to be surprisingly small but the product $(s\tau)_e$ has the order of magnitude expected from our previous studies of charging of dust particles.

Keywords: Plasma-material interaction, electron states at surfaces

1. Introduction

Recently, we proposed a surface model for the charge of a dust particle in a plasma which avoids the unrealistic treatment of the grain surface as a perfect absorber for electrons and ions [1]. The charging of the dust particle is instead described as a physisorption process in the potential of the distorted region of the grain. Since the grain is negatively charged, this potential is for ions attractive on all length scales. For electrons, however, it becomes attractive only at extremely small distances, where the attractive polarization-induced part of the potential dominates the Coulomb repulsion.

Provided ions get stuck in the attractive Coulomb tail of the grain potential, in trapped orbits, a few μm away form the grain surface, the grain charge is just the number of electrons quasi-bound in the states of the polarization-induced part of the electron-grain interaction. Encapsulating the microphysics responsible for sticking into and desorption from these states into a sticking coefficient s_e and a desorption time τ_e an estimate for this number can be obtained by balancing on the grain surface the electron collection flux with the electron desorption flux. As a result [1],

$$Z_p = 4\pi R^2 s_e \tau_e j_e^{\rm OML}(Z_p) \; , \tag{1}$$

where the electron plasma flux is given by the orbital-motion limited electron flux and R is the grain radius.

In [1] we invoked the phenomenology of reaction rate theory to directly approximate the product $s_e\tau_e$ by an Arrhenius-like expression,

$$s_e\tau_e = \frac{h}{k_B T_s} \exp\left[\frac{E_e^d}{k_B T_s}\right] \; , \tag{2}$$

containing the electron desorption energy E_e^d and the grain surface temperature T_s as parameters. Identifying $-E_e^d$ with the binding energy of the lowest polarization-induced (image) state and using T_s, due to lack of experimental data, as an adjustable parameter, we obtained excellent agreement with experimentally measured grain charges [1, 2]. For a μm-sized grain in a typical low-temperature gas discharge $s_e\tau_e \approx 10^{-6} s$.

The assumptions on which our model is based – ions not reaching the grain surface on the microscopic scale, instead quasi-bound a few μm in front of the grain surface, and electrons quasi-bound in external polarization-induced surface states – can be only justified by a complete microscopic calculation. The most pressing issues in this respect are a selfconsistent calculation of the ion density surrounding a negatively charged grain and an explicit calculation of $s_e\tau_e$ from a microscopic model for the electron-grain interaction. In the following we present first results for the latter. A full description of our approach will be given elsewhere [3].

2. Calculational scheme

As explained in [3], for the calculation of s_e and τ_e it suffices to consider, in a first approximation, a planar, uncharged plasma boundary. It defines the xy-plane of a coordinate system separating the plasma in the halfspace $z > 0$ from the solid in the halfspace $z \leq 0$.

The microphysics of electrons at an idealized metallic boundary, where the only surface modification due to the plasma is the build-up of surface charges, is schematically shown in Fig. 1. A plasma electron approaching the boundary in an extended state with $E > 0$ may be bound in a surface state with $E < 0$ provided it dissipates its excess energy to the internal electron-hole pairs of the metallic boundary. Similarly, an electron initially occupying a bound surface state may desorb from the surface when it gains enough energy to reach an extended state.

Quite generally, a quantum-mechanical calculation of the electron sticking coefficient and electron desorp-

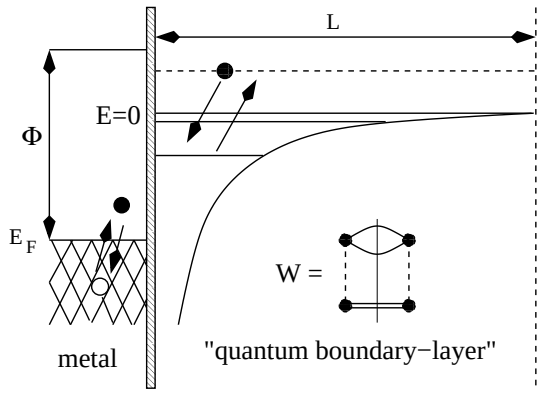

Fig. 1: Illustration of the microphysics of plasma electrons at metallic boundaries. L is the width of the "boundary layer" where a quantum-mechanical calculation applies; Φ and E_F are, respectively, the work function and the Fermi energy of the metal.

tion time has to be based on a Hamiltonian,

$$H = H_e + H_b + H_{e-b} \ , \tag{3}$$

where H_e and H_b describe, respectively, the unperturbed dynamics of plasma electrons in the vicinity of the solid and of elementary excitations of the solid responsible for electron energy relaxation and H_{e-b} encodes the coupling between the two.

The electronic structure of a plasma boundary is rather complex. For instance, it cannot be expected that the boundary coincides with a crystallographic plane. More likely, the boundary is polycrystalline and consists of an irregular array of terraces. In addition, it may be chemically modified due to the plasma. As a first step, however, we nevertheless assume a perfect boundary. The model may be applicable when the size of terraces is large and the chemical contamination is negligibly small.

Even then two types of surface states are possible and should be included in H_b: Crystal-induced states due to the abrupt appearance of a periodic potential for $z \leq 0$ and polarization-induced (image) states due to quantum-mechanical exchange and correlation effects for $z > 0$. The former states are rather close to the surface whereas the latter extend deep into the plasma. Our exploratory calculation contains therefore only image states. To keep the mathematics as simple as possible we approximated moreover these states by classical image states, although this is not quite correct for the distances we are interested in. The wavefunctions for the approaching plasma electron are then Whittaker functions [3].

As already mentioned, for metallic surfaces, the creation and annihilation of internal electron-hole pairs due to the Coulomb interaction between plasma and metal electrons is the main energy relaxation channel. To include this process we describe the metallic boundary by a Jellium halfspace [4, 5] interacting with the electrons of the plasma via a screened Coulomb interaction: $V_s(r) \sim \exp[-(k_s)_{\rm surface} r]/r$, where $(k_s)_{\rm surface}$ is the screening wavenumber at the surface. To be consistent with the classical image states we have to assume an infinitely high barrier at $z = 0$. The wavefunctions for internal electrons are then standing waves and the coupling matrix elements entering H_{e-b} can be worked out analytically [3].

metal	$E_F[eV]$	$k_F[\mathring{A}]$	$(k_s)_{\rm bulk}/k_F$
Cu	7.0	1.36	1.33
Al	11.7	1.75	1.17
Be	14.3	1.94	1.11

Table 1: Fermi energy E_F, Fermi wavenumber k_F, and screening wavenumber $(k_s)_{\rm bulk}$ for various metals [6].

If the desorption time is sufficiently long, plasma electrons bound in image states are in thermal equilibrium with the surface. The inverse of the electron desorption time, the desorption rate, is then given by [3,7]

$$\frac{1}{\tau_e} = \frac{\sum_{\vec{Q}'n'} \sum_{\vec{Q}q} \exp[-\beta_s E_{\vec{Q}'n'}] \mathcal{W}(\vec{Q}q, \vec{Q}'n')}{\sum_{\vec{Q}n} \exp[-\beta_s E_{\vec{Q}n}]} \ , \tag{4}$$

where $T_s = (k_B \beta_s)^{-1}$ is the surface temperature and $\mathcal{W}(\vec{Q}q, \vec{Q}'n')$ is the transition rate from the bound surface state $(\vec{Q}', n')$, with $\vec{Q}'$ the lateral momentum and n' the vertical quantum number, to the extended surface state $(\vec{Q}, q)$. The energy of the two states is, respectively, $E_{n\vec{Q}}$ and $E_{q'\vec{Q}'}$.

For the results presented below the transition rate $\mathcal{W}(\vec{Q}q, \vec{Q}'n')$ was calculated from the Hamiltonian (3) perturbatively as shown in Fig. 1. This is equivalent to a golden rule calculation of the transition rate and leads to (q and q' may label bound and extended surface states)

$$\begin{aligned} \mathcal{W}(\vec{Q}q, \vec{Q}'q') = \frac{2\pi}{\hbar} \sum_{\vec{K}\vec{K}'} \sum_{kk'} |\mathcal{V}^{\vec{Q}q \ \vec{K}k}_{\vec{Q}'q' \vec{K}'k'}|^2 \\ \times \ n_F(E_{\vec{K}'k'})[1 - n_F(E_{\vec{K}k})] \\ \times \ \delta(E_{\vec{Q}'q'} + E_{\vec{K}'k'} - E_{\vec{Q}q} - E_{\vec{K}k}) \ , \end{aligned} \tag{5}$$

where $n_F(E) = 1/(\exp[(E - E_F)/k_B T_s] + 1)$ is the Fermi distribution function for the metal electrons with Fermi energy E_F and temperature T_s, $\mathcal{V}^{\vec{Q}q \ \vec{K}k}_{\vec{Q}'q' \vec{K}'k'}$ is the Coulomb matrix element describing the scattering of a plasma electron initially in state $(\vec{Q}', q')$ on a metal electron initially in state $(\vec{K}', k')$, and $E_{\vec{K}',k'}$ is the energy of the electron in the metal.

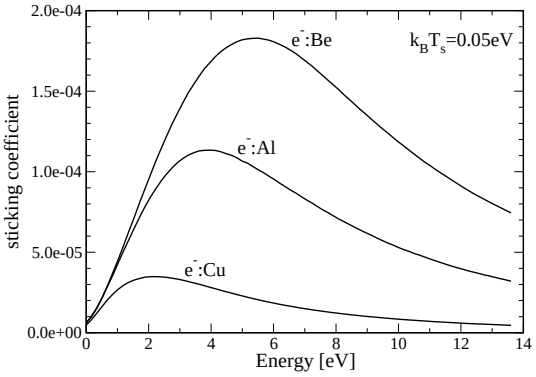

Fig. 2: Energy resolved sticking coefficient for plasma electrons hitting perpendicularly, respectively, a copper, an aluminum, and a beryllium surface at $k_B T_s = 0.05eV$.

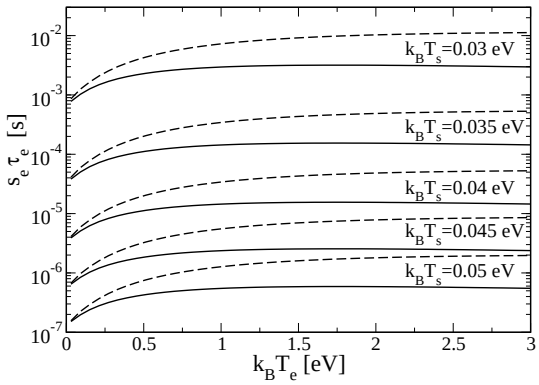

Fig. 3: The product $s_e\tau_e$ as a function of $k_B T_e$ for a thermal beam of plasma electrons hitting, respectively, a copper (full line) and a beryllium (dashed line) surface at various temperatures $k_B T_s$.

For an electron in an extended surface state the tendency to stick to any bound surface state is [3, 8]

$$S_{\vec{Q}'q'} = \frac{16Lm_e}{\hbar q'} \sum_{\vec{Q}n} \mathcal{W}(\vec{Q}n, \vec{Q}'q') \ , \qquad (6)$$

where L is the width of the quantum-mechanical boundary layer (which drops out in the limit $L \to \infty$), m_e is the electron mass, and $\mathcal{W}(\vec{Q}n, \vec{Q}'q')$ is the transition rate from the extended surface state $(\vec{Q}', q')$ to the bound surface state $(\vec{Q}, n)$. Provided extended surface states are Maxwellian occupied, with a temperature $T_e = (k_B\beta_e)^{-1}$, the angle and energy averaged sticking coefficient – the global sticking coefficient – is

$$s_e = \frac{\sum_{\vec{Q}'q'} S_{\vec{Q}'q'} q' \exp[-\beta_e E_{\vec{Q}'q'}]}{\sum_{\vec{Q}'q'} q' \exp[-\beta_e E_{\vec{Q}'q'}]} \ . \qquad (7)$$

Subject to the constraints of the perturbative calculation of the transition rates, the functional form of Eqs. (4)–(7) is generic. With transition rates and single particle energies calculated from an appropriate microscopic model these formulas could be also applied to non-metallic boundaries.

3. Results

Before we discuss numerical results for the electron sticking coefficient and desorption time let us add a few remarks about the screening wavenumber $(k_s)_{\rm surface}$. Little is known about this parameter except that it should be smaller than the bulk screening wavenumber $(k_s)_{\rm bulk}$ because the electron density close to the surface is smaller than in the bulk of the material. A microscopic calculation of $(k_s)_{\rm surface}$ is a complicated manybody problem beyond the scope of the present study. For it it suffices to recall that in [4] it was argued, based on a comparison of experimentally and theoretically obtained branching ratios for positron trapping at and transmission through metal surfaces that most probably $(k_s)_{\rm surface} = 0.6(k_s)_{\rm bulk}$. For the results presented below we used therefore this value for $(k_s)_{\rm surface}$ with the respective bulk screening wavenumbers given in table 1.

In addition we modified the binding energies of the surface states as obtained from the classical image potential by an overall factor of 0.7. This factor was chosen to bring the binding energy of the lowest surface state $|E_1| = 0.85eV$ in accordance with the experimentally measured value for copper: $|E_1|^{\rm Cu} \approx 0.6eV$ [9]. Assuming this modification to approximately account for the deviation of the true polarization-induced potential from the classical image potential, we used this value also for the other metals.

Figure 2 shows the energy resolved sticking coefficient when the plasma electron perpendicularly hits, respectively, a copper, an aluminum, and a beryllium boundary at $kT_s = 0.05eV$. Proviso the assumptions we made about the electronic structure of the plasma boundary and the modifications of the binding energies and the screening parameter, the sticking coefficient turns out to be extremely small, of the order of $10^{-5} - 10^{-4}$. For weaker screening, and thus stronger coupling, we would obtain sticking coefficients as large as 10^{-1} but these screening wavenumbers are unphysical. Global sticking coefficients defined in (7) are also very small (see table 2). Although we cannot rule out that this is an artifact of our model, in particular, of our neglect of crystal-induced surface states, we also point out that the basis of the widely accepted values $s_e \approx 0.1 - 1$ seems to be a semiclassical back-on-the-envelop approximation [10] which does not withstand critical analysis. In addition, the expression for the sticking coefficient derived in [10] gives, for electron temperatures and binding energies typical for grains

	Cu	Al	Be
$\tau_e[s]$	0.026	0.021	0.022
$s_e[10^{-5}]$	1.8	5.6	8.9
$s_e\tau_e[10^{-6}s]$	0.46	1.19	1.95

Table 2: Electron desorption time and global sticking coefficient for a thermal beam of plasma electrons with $k_BT_e = 5eV$ hitting various metal surfaces at $k_BT_s = 0.05eV$.

in dusty laboratory plasmas, even smaller values than the ones we obtain from our quantum-mechanical approach [3].

Desorption times τ_e obtained from Eq. (4) are of the order of $10^{-2}s$ (see table 2). Within our model, they are almost independent of the electron temperature. But, through the Boltzmann factor, they depend strongly on the surface temperature. Since for the charging model described in the introduction the product $s_e\tau_e$ is of central importance, we do not present data for τ_e individually. Instead we plot in Fig. 3 for thermal electrons hitting, respectively, a copper and a beryllium surface, the product $s_e\tau_e$. It also depends strongly on the surface temperature and weakly on the electron temperature. Although the sticking coefficient is in contradiction to what is generally assumed, the product $s_e\tau_e$ has the order of magnitude expected from our surface model. Indeed, the values of $s_e\tau_e$ for $kT_s \approx 0.05eV$ would produce charges for μm-sized metallic grains of the correct order of magnitude. This is not a proof for our model. But it is nevertheless reassuring that the microscopic calculation produces for not too unrealistic assumptions $s_e\tau_e$ values consistent with the phenomenological approach adopted in [1].

Let us finally mention that the phenomenological expression (2) used in [1] cannot be rigorously obtained from Eqs. (4) and (7). However, keeping only a single bound state and assuming both the surface and the "relevant "electron temperature, which is not necessarily the electron temperature in the bulk of the discharge (see discussion in [1]), to be much smaller than the binding energy of this state, we can apply Laplace's approximation to the integrals (4) and (7) to obtain [3]

$$s_e^L\tau_e^L = \frac{16h}{(k_BT_s)^{3/2}(k_B\tilde{T}_e)^{-1/2}}\exp[\beta_s|E_1|]\ , \qquad (8)$$

which is identical to Eq. (2) when the relevant electron temperature $\tilde{T}_e$ is of the order of the surface temperature. The numerical factor $16 = 8 \times 2$, which is absent in Eq. (2), is a consequence of the asymptotic form of the extended states of the classical image potential (factor 8) and of the fact that an electron approaching the grain boundary in an extended state can make a transition to any bound state on its way towards the surface and on its way back to the plasma (factor 2).

4. Concluding remarks

To support our surface model for the charge of a μm-sized grain in a gas discharge, which avoids treating the grain as a perfect absorber for electrons and ions and describes the build-up of surface charges as a physisorption process in the disturbed region of the grain, we investigated the microphysics of electrons at plasma boundaries. Specifically, we calculated for a metallic boundary the electron sticking coefficient s_e and the electron desorption time τ_e assuming physisorption of electrons at metals to be controlled by electron-hole pair induced transitions between classical image states. Within this model, the sticking coefficient is unexpectedly small, $s_e \approx 10^{-4}$, indicating that the model is perhaps incomplete. In particular, the neglect of crystal-induced surface states may be critical. On the other hand, the product $s_e\tau_e \approx 10^{-6}s$ for $kT_s \approx 0.05eV$, which is the order of magnitude we would need to reproduce, for typical discharge conditions, the charge of a μm-sized metallic grain. Further studies are thus clearly needed to develop a consistent microscopic theory of particle charging.

Acknowledgment

Support from the SFB-TR 24 "Complex Plasmas" is greatly acknowledged.

References

[1] F. X. Bronold, H. Fehske, H. Kersten, H. Deutsch, Phys. Rev. Lett. **101** (2008) 175002.

[2] F. X. Bronold, H. Fehske, H. Kersten, H. Deutsch, accepted by Contrib. Plasma Phys. (2009); arXiv:0904.3187.

[3] F. X. Bronold, H. Fehske, H. Deutsch, arXiv:0901.4915 (2009).

[4] D. Neilson, R. M. Nieminen, J. Szymański, Phys. Rev. B **33** (1986) 1567.

[5] A. B. Walker, K. O. Jensen, J. Szymański, D. Neilson, Phys. Rev. B **46** (1992) 1687.

[6] N. W. Ashcroft, N. D. Mermin, Solid State Physics (Holt, Rinehart and Winston, New York) (1976).

[7] H. J. Kreuzer, Z. W. Gortel, Physisorption Kinetics (Springer Verlag, Berlin) (1986).

[8] Z. W. Gortel, J. Szymański, Phys. Rev. B **43** (1991) 1919.

[9] A. Elmahboubi, Y. Lépine, Solid State Commun. **94** (1995) 655.

[10] T. Umebayashi, T. Nakano, Publ. Astron. Soc. Japan **32** (1980) 405.